JOURNAL OF BACTERIOLOGY, Jan. 1996, p. 248–257 Vol. 178, No. 1
0021-9193/96/$04.00+0

Molecular and Phylogenetic Characterization of Pyruvate and 2-Ketoisovalerate Ferredoxin Oxidoreductases from *Pyrococcus furiosus* and Pyruvate Ferredoxin Oxidoreductase from *Thermotoga maritima*

ARNULF KLETZIN† AND MICHAEL W. W. ADAMS*

Department of Biochemistry and Center for Metalloenzyme Studies, University of Georgia, Athens, Georgia 30602

Received 19 June 1995/Accepted 2 November 1995

Previous studies have shown that the hyperthermophilic archaeon *Pyrococcus furiosus* contains four distinct cytoplasmic 2-ketoacid oxidoreductases (ORs) which differ in their substrate specificities, while the hyperthermophilic bacterium *Thermotoga maritima* contains only one, pyruvate ferredoxin oxidoreductase (POR). These enzymes catalyze the synthesis of the acyl (or aryl) coenzyme A derivative in a thiamine PP_i-dependent oxidative decarboxylation reaction with reduction of ferredoxin. We report here on the molecular analysis of the POR (*por*) and 2-ketoisovalerate ferredoxin oxidoreductase (*vor*) genes from *P. furiosus* and of the POR gene from *T. maritima*, all of which comprise four different subunits. The operon organization for *P. furiosus* POR and VOR was *porG-vorDAB-porDAB*, wherein the γ subunit is shared by the two enzymes. The operon organization for *T. maritima* POR was *porGDAB*. The three enzymes were 46 to 53% identical at the amino acid level. Their δ subunits each contained two ferredoxin-type [4Fe-4S] cluster binding motifs (CXXCXXC XXXCP), while their β subunits each contained four conserved cysteines in addition to a thiamine PP_i-binding domain. Amino-terminal sequence comparisons show that POR, VOR, indolepyruvate OR, and 2-ketoglutarate OR of *P. furiosus* all belong to a phylogenetically homologous OR family. Moreover, the single-subunit pyruvate ORs from mesophilic and moderately thermophilic bacteria and from an amitochondriate eucaryote each contain four domains which are phylogenetically homologous to the four subunits of the hyperthermophilic ORs (27% sequence identity). Three of these subunits are also homologous to the dimeric POR from a mesophilic archaeon, *Halobacterium halobium* (21% identity). A model is proposed to account for the observed phenotypes based on genomic rearrangements of four ancestral OR subunits.

The final oxidative step in the fermentation of carbohydrates in anaerobic microorganisms is typically catalyzed by pyruvate ferredoxin oxidoreductase (POR). This involves the oxidative decarboxylation of pyruvate with the participation of thiamine PP_i (TPP) followed by the transfer of an acetyl moiety to coenzyme A (CoASH) for the synthesis of acetyl-CoA as shown in the following equation: CH_3-CO-COOH + CoASH → CH_3-CO-SCoA + CO_2 + $2H^+$ + $2e^-$ (e^- is an electron) (44, 45). The electrons from this reaction are transferred to low-potential ferredoxins or flavodoxins typically for ultimate disposal either as H_2 or in an organic compound.

PORs have been purified from several anaerobic hyperthermophiles, which are organisms that grow at temperatures near and above 100°C (42). These include the sulfur-reducing archaea *Pyrococcus furiosus* (6) and *Thermococcus litoralis* (15), the sulfate-reducing archaeon *Archaeoglobus fulgidus* (28), and the bacterium *Thermotoga maritima* (7). All the hyperthermophilic PORs comprise four different subunits (α, β, γ, and δ) with apparent molecular masses of approximately 43, 35, 23, and 12 kDa, respectively. We have also purified three other types of 2-ketoacid-oxidizing, CoASH-dependent oxidoreductases (ORs) from *P. furiosus* and *T. litoralis*; however, they do not occur in *T. maritima*. These are involved in peptide fermentation and oxidize the transaminated forms of various amino acids. 2-Ketoisovalerate OR (VOR) oxidizes predominantly branched-chain 2-ketoacids, which are derived from valine, leucine, and isoleucine (17, 22); 2-ketoglutarate OR (KGOR) is specific for 2-ketoglutarate (22, 32); and indolepyruvate OR (IOR) preferentially oxidizes 2-keto acids generated from the aromatic amino acids (31). VOR and KGOR also contain four distinct subunits with sizes comparable to those of the PORs, whereas IOR consists only of two subunits (A and B) with sizes of 66 and 23 kDa (17, 31, 32). As with POR, the acyl- and aryl-CoA derivatives produced by the three other ORs are thought to be utilized for energy conservation (1a, 2, 22).

PORs have also been purified from various mesophilic organisms, including several anaerobic bacteria (8, 20, 33, 37, 44, 45), aerobic archaeal halobacteria (23, 24, 38), and anaerobic eucaryotes (10, 47). On the other hand, in most aerobic organisms, pyruvate oxidation is catalyzed by a pyruvate dehydrogenase (PDH) complex (reviewed in reference 46). The reactions catalyzed by PDH and the ORs (POR, VOR, KGOR, and IOR) involve both the formation of an acyl-TPP complex and the transfer of the acyl moiety to CoASH, but PDH differs in the use of NAD as an electron acceptor and in the presence of lipoic acid and flavin but the absence of iron-sulfur (FeS) clusters. The mechanism of pyruvate oxidation by PDH has been firmly established, but this is not the case with the ORs. For example, TPP radical-based (24, 37, 41) and non-radical-based (41, 45) reactions have been proposed, and it is not clear

* Corresponding author. Mailing address: Department of Biochemistry, Life Sciences Building, University of Georgia, Athens, GA 30602. Phone: (706) 542-2060. Fax: (706) 542-0229. Electronic mail address: ADAMSM@BSCR.UGA.EDU.

† Present address: Institut für Mikrobiologie, Technische Hochschule Darmstadt, 64287 Darmstadt, Germany.

how acyl transfer to CoASH takes place in the ORs without lipoic acid. It has been suggested that an FeS cluster acts as an intermediate binding site for the acyl moiety, although the precise mechanism is unclear (37, 41, 45). Moreover, the exact role and, in many cases, the actual number of FeS clusters in the ORs are uncertain (see, for example, reference 7).

In contrast to the four-subunit structure of the ORs from the hyperthermophilic archaea (1a, 2, 7, 22) and hyperthermophilic bacteria (7), most PORs of mesophilic bacteria and of eucaryotic protozoans are homodimers, and the primary structures for several are known (4, 5, 9, 18, 26). Each subunit (125 kDa) is about the size of the four subunits of the hyperthermophilic ORs combined and contains between one and three FeS clusters and one TPP molecule. A notable exception is the four-subunit POR from the mesophilic bacterium *Helicobacter pylori*, which so far is the only example of this type in a mesophile (20). In further contrast, the POR from the aerobic halophilic archaeon *Halobacterium halobium* consists of two different subunits (68 and 35 kDa) and contains only one FeS cluster per dimer (24, 38). Even in the absence of complete sequences for the multisubunit hyperthermophilic ORs, it has been suggested that they and the single-subunit PORs are phylogenetically related (17, 18, 20, 28). Herein we report the first *por* operons to be sequenced from the hyperthermophiles together with the first *vor* operon to be sequenced from any organism. We show that all of the hyperthermophilic and mesophilic ORs are phylogenetically homologous. This includes *H. halobium* POR, which has resisted any previous attempt at meaningful classification. We show that the different subunit structures observed for these enzymes can be explained by operon rearrangements of an ancestral OR of four subunits.

MATERIALS AND METHODS

Organisms and DNA preparation. *P. furiosus* (DSM 3638) (11) and *T. maritima* (DSM 3109) (19) were grown according to published procedures (11, 19, 21). DNA was prepared by the cetyl trimethyl ammonium bromide (CTAB) method with CsCl purification as described elsewhere (48).

Cloning, subcloning, and sequencing of the *P. furiosus por* and *vor* genes. From the N-terminal amino acid sequence of each of the subunits of *P. furiosus* POR, a pair of oligonucleotides, one each from the coding and anticoding strands, was designed (see Fig. 1). For lack of significant codon usage tables for both organisms, the following rules were applied for wobble positions of codons. For N (any base), inosine was chosen regardless of the position in the oligonucleotides. Within the last 9 bases of the 3′ end a degenerate mix of G and A (for purines), T and C (for pyrimidines), and A, T, and C (for the isoleucine codons) was included. Within the remaining part of the oligonucleotides (11 to 14 bases) G was chosen for purines, T was chosen for pyrimidines, and a degenerate mix of A and T was chosen for isoleucine, assuming a reasonable GT base pairing in the case of a wrong match. Custom oligonucleotides were obtained from Stratagene. All meaningful combinations of oligonucleotides from different subunits were chosen for PCR amplification of intervening parts of the operon. The initial annealing temperature of 37°C in PCR was shifted after the third cycle to 54°C and kept for the remaining 35 cycles. Following visualization on agarose gels, unique bands were excised and cloned into the pCRscript vector (Stratagene) according to the manufacturer's instructions. Sequencing of two different clones showed that one (pPP6; see Fig. 2) contained a 385-bp fragment coding for the δ subunit and the N terminus of the α subunit, while the second contained an overlapping fragment coding for the N terminus of the δ subunit and 785 bp upstream (because of nonspecific binding of the second A-subunit oligonucleotide) (pPP5; see Fig. 2). In addition, the two oligonucleotides derived from the γ subunit were used for the amplification, cloning, and sequencing of a 59-bp fragment specific for that subunit (pPP-G). For probe generation, the gel-purified pPP6 fragment was subjected to a second round of PCR amplification with the same set of oligonucleotides and the labeling mix contained in the digoxigenin labeling kit (Boehringer) diluted fivefold with unlabeled deoxynucleoside triphosphates (dNTPs) (0.2 mM final concentration of dNTPs). Following digestion of genomic DNA, Southern hybridization was carried out according to standard procedures (40), with luminescence detection according to the manufacturer's instructions. An internal oligonucleotide derived from the sequence was labeled with polynucleotide kinase and [γ-^{32}P]ATP according to standard procedures (40) and was used for the identification of positive clones following colony lifting. A 2,675-bp *Pst*I fragment which contained the genetic information for the δ subunit and the first 72 amino acid residues of the α subunit of POR and, upstream, the α subunit (except for the first 13 amino acid residues) and the entire β subunit of *P. furiosus* VOR (pPP23; see Fig. 2) was identified and cloned into pUC19. The downstream part of the POR operon was cloned in a similar fashion by using the same ^{32}P-labeled oligonucleotide to identify and clone a 2,939-bp overlapping *Xho*I-*Eco*RV fragment into pBluescript II KS$^+$ cut with the same enzymes (pPP24; see Fig. 2). To clone the upstream part of the VOR operon, including the shared γ subunit, an oligonucleotide derived from the sequence of the upstream end of pPP23 was used in addition to the [α-^{32}P]dATP PCR-labeled insert of pPP-G. Both probes gave identical patterns in Southern hybridization except with the restriction enzyme *Pst*I (see Fig. 2), suggesting that the missing POR γ subunit was indeed coded upstream of VOR. In the course of cloning a 5,317-bp overlapping *Kpn*I-*Eco*RV fragment into both pBluescript II KS$^+$ (pPP25) and pBluescript II SK$^+$ (pPP26), a third positive clone (pPP27, 3,418 bp; see Fig. 2) which was the product of a random truncation of the original fragment on the side of the blunt-ended *Eco*RV site was found. The sequencing of the entire 9,585-bp single *Eco*RV fragment was carried out by a mixture of primer walking and the construction, cloning, and sequencing of nested deletions. Double-stranded sequencing was used in each case with the original plasmids or one of the deletion clones as a template. New sequencing primers were derived from previously determined parts, from flanking regions of the original clone, or from the deletion plasmids with T3 and T7 primers (for pBluescript; Stratagene) or M13 universal and reverse primers (for pUC). All sequencing was carried out by the dideoxy chain termination method using the Sequenase kit (United States Biochemical Corp.) with [α-^{35}S]dATP (Amersham) according to the manufacturer's instructions. Sequencing reactions were run in the BaseAce sequencing apparatus (Stratagene).

Cloning, subcloning, sequencing, and expression of the *T. maritima por* gene. The *T. maritima por* gene was cloned in a fashion similar to that used for the *P. furiosus por* and *vor* genes. The combination of an oligonucleotide from the α subunit with one from the β subunit resulted in the cloning of a unique 639-bp PCR-amplified fragment into pCRscript due to arbitrary priming of the β-subunit oligonucleotide. From sequencing, it was shown to contain the information for the C-terminal part of the γ subunit, the entire δ subunit, and the N terminus of the α subunit. Probe generation, cloning, and sequencing were done as described above. A 4,030-bp *Hin*dIII-*Pst*I fragment was cloned into pUC18 (pHP 511) and later into pBluescript II KS$^+$ (pKSHP) and was sequenced. This contained the C-terminal half of the γ subunit and all of δ, α, and β subunits, as well as a gene downstream encoding a putative glucose dehydrogenase (*gld*) or an oxoacyl carrier protein reductase (*fabG*). For the upstream part of the *por* operon, an overlapping 3,418-bp *Bam*HI fragment was cloned into pBluescript II KS$^-$ (pKB-112) and sequenced. In addition to the entire γ subunit, the upstream fragment contained a putative methyl-accepting chemotaxis protein and the C-terminal part of a CDP-abequose synthase (see Fig. 2).

Sequence comparisons and phylogenetic analysis. The searches in the NBRF, the Swiss Prot, the combined GenBank-EMBL, and the PROSITE databases for sequence similarities were carried out with the programs FASTA, TFASTA, BLAST, and MOTIFS (University of Wisconsin Genetics Computer Group; version 8.0). The sequences of the *nifJ* gene products of an *Anabaena* sp. (accession number L14925 [5]), *Rhodospirillum rubrum* (X77515 [5]), *Klebsiella pneumoniae* (X13109 and X13303 [4, 9]), and *Enterobacter agglomerans* (X78558 [26]); *Trichomonas vaginalis* POR A and B (U16822 and U16823 [18]); and the *H. halobium por* product (X64521 and X22397 [38]) were extracted from the databases and subjected to specific sequence comparisons to the POR and VOR amino acid sequences with the programs GAP, FASTA, and WORDSEARCH (University of Wisconsin Genetics Computer Group). Pairwise alignments were done in a modified way as described earlier (25) with the program GAP (gap weight = 3), and the resulting percent identities, percent similarities, alignment scores (quality [*A*]), mean random alignment scores (*R*), and standard deviations (SD; $n = 20$) were recorded. The product of $(A - R)$/SD was calculated as a measure of the significance of the alignment results (Table 1) (25), wherein values greater than 10 were considered significant. For the pairwise comparisons and for the multiple alignments, the sequences of *P. furiosus* POR and VOR and of *H. halobium* POR were put together into a contiguous sequence file in the order present in the single-subunit PORs. Because of the absence of the δ domain in the large subunit of the *H. halobium* POR sequence (see below) and the low overall similarity, the computer programs did not find the optimal alignment in an unbiased search. For this reason, a second alignment was conducted with the sequences as aligned in Fig. 3 and 4 under more stringent conditions (gap weight = 10) to avoid the introduction of secondary gaps. Multiple alignments were carried with the programs PILEUP and LINEUP, and these were manually corrected against the results of pairwise alignments, multiple alignments of subsets of the sequences, and conserved signatures not found by the computer programs. The phylogenetic dendrogram was calculated with the programs DISTANCES and GROWTREE (University of Wisconsin Genetics Computer Group), and branch length corrections were included.

Nucleotide sequence accession numbers. Nucleotide sequences were submitted to the EMBL data library; the accession numbers assigned were X85250 for the *P. furiosus por* and *vor* genes and X85171 for *T. maritima por.*

TABLE 1. Pairwise comparison of 2-ketoacid ORs[a]

	As	Rr	Kp	Ea	Tv A	Tv B	Pf P	Pf V	Tm	Hh
Anabaena sp. POR	241.2	57.7	49.7	49.7	43.9	43.6	**27.7**	**27.2**	**27.3**	19.7
R. rubrum POR	136.9	236.9	49.1	48.4	44.3	44.2	**27.6**	**29.3**	**26.9**	21.1
K. pneumoniae POR	111.9	108.9	234.2	71.7	44.3	44.1	**27.5**	**27.5**	**27.4**	20.4
E. agglomerans POR	110.7	106.8	172.0	236.4	45.7	45.4	**26.4**	**29.0**	**29.7**	19.8
T. vaginalis POR A	96.2	95.8	101.0	100.9	234.6	94.5	**27.9**	**27.3**	**25.5**	18.3
T. vaginalis POR B	95.9	94.7	100.4	99.7	224.8	234.1	**27.9**	**27.6**	**25.5**	19.4
***P. furiosus* POR**	**22.1**	**25.4**	**26.6**	**26.1**	**23.3**	**23.4**	**203.0**	**53.6**[b]	**45.5**	**17.7**
***P. furiosus* VOR**	**24.2**	**28.7**	**25.8**	**26.9**	**24.2**	**23.7**	**113.6**	**199.6**	**44.7**	**16.8**
***T. maritima* POR**	**26.4**	**28.0**	**27.5**	**29.8**	**25.8**	**26.3**	**80.6**	**79.2**	**202.6**	**17.7**
H. halobium POR[c]	2.3/ 24.8	4.8/ 27.4	1.6/ 26.1	0.8/ 26.1	3.6/ 24.7	3.8/ 24.5	**6.1/ 39.3**	**2.9/ 38.3**	**5.2/ 37.1**	186.7/ 176.5

[a] The available sequences of ORs were combined into a single file in the order given in the alignments (Fig. 3 and 4). The upper right triangle shows pairwise identities, and the lower left triangle depicts the significance evaluation of the alignment results. The values for *P. furiosus* POR, *P. furiosus* VOR, and *T. maritima* POR are shown in boldface. The significance evaluation value is a measure of the significance of the alignment results and is the product of $(A - R)$/SD from an unbiased alignment where A is the alignment score (quality), R is the mean random alignment score, and SD is the standard deviation ($n = 20$). *As* and *Rr*, etc., are abbreviations for the respective species given in the left column.

[b] The percent identity of *P. furiosus* POR and VOR does not include the shared γ subunit.

[c] In the case of *H. halobium* POR, the program did not find the optimal alignments because of the low overall similarity, so the procedure was repeated with the sequences aligned as given in Fig. 3 and 4 with gaps included applying high stringency (gap weight = 10). When the same procedure was applied to *P. furiosus* POR and VOR and *T. maritima* POR in comparison with the single-subunit ORs, the scores were approximately double the values of those shown. For comparison, an optimal alignment with randomly selected, unrelated protein sequences gave values between 5 and 15 with this method. For references, accession numbers, and a more detailed description, see Materials and Methods.

RESULTS AND DISCUSSION

Amino-terminal sequences and the generation of probes. Amino-terminal sequences for the subunits of POR (6), IOR (31), and VOR (2, 17) from *P. furiosus*; POR (15), IOR (32), VOR (17), and KGOR (2, 22, 32) from *T. litoralis* (35); and POR (7, 31) from the hyperthermophilic bacterium *T. maritima* are shown in Fig. 1. Each of the enzymes comprises four subunits (α, β, γ, and δ), with the exception of the IORs, which comprise two subunits (A and B). The multiple alignment (Fig. 1) showed that the sequence for a given subunit from one enzyme is homologous to those of the same subunit type from the other enzymes, except for the γ subunit of *T. maritima* POR (7, 31). This prompted a redetermination of its amino-terminal sequence, and the new sequence proved to be similar to those of the other γ subunits (Fig. 1). Notably, the γ subunits of POR and VOR from *P. furiosus* have the same amino-terminal sequence. In addition, the large subunit (A) of the IORs from *P. furiosus* and *T. litoralis* are homologous to the α subunits of POR, VOR, and KGOR, and the small IOR subunit (B) is homologous to the γ subunits of the other ORs (Fig. 1). The four subunits of the POR from the mesophilic bacterium *H. pylori* are also homologous to the respective subunits of the PORs from the hyperthermophiles (20). Moreover, the amino terminus of the large subunit (a) of *H. halobium* is homologous to the γ subunits of the hyperthermophilic ORs (Fig. 1). It had been previously reported that the small subunit (b) of *H. halobium* POR is homologous to the β subunit (18, 28). Clearly, the four subunits of the various hyperthermophilic ORs are closely related, and a relationship to *H. halobium* POR is also suggested by the data. Of a set of meaningful pairwise combinations of oligonucleotides derived from the amino termini of different subunits of *P. furiosus* and *T. maritima* PORs (Fig. 1), three were successful in PCR amplification of parts of the respective operons (pTm-3, pPP-6, and pPP-5; Fig. 2).

***P. furiosus por* and *vor*.** Southern hybridization of genomic digests of *P. furiosus* DNA probed with the pPP-6 insert encoding the δ subunit of POR consistently identified one major and three to four minor bands even after application of the most stringent washing conditions (65°C, 0.1× SSC [1× SSC is 0.15 M NaCl plus 0.015 M sodium citrate]), suggesting the presence of other ORs in *P. furiosus*. The initially identified and cloned 2,675-bp *Pst*I fragment (pPP23) contained the δ subunit of POR, the first 72 amino acid residues of the α subunit, and upstream, to our surprise, the α and β subunits of *P. furiosus* VOR (Fig. 2). Subsequently, on the downstream *Xho*I-*Eco*RV fragment (pPP24; Fig. 2) and the upstream *Kpn*I-*Eco*RV fragment (pPP25), the remaining parts of the POR and VOR operons were cloned, such that the three plasmids were contained within a single large 9,585-bp *Eco*RV fragment, the sequence of which was determined completely on both strands. This fragment contained the entire genetic information for the subunits of POR and VOR in three separate units in the order (i) *porG*, encoding the shared γ subunit of POR and VOR; (ii) *vorD*, *vorA*, and *vorB*; and (iii) *porD*, *porA*, and *porB*. The complete amino acid sequences are given in the Fig. 3 (α and γ) and 4 (δ and β) together with those of *T. maritima*, *H. halobium*, and *K. pneumoniae* PORs. Amino-terminal residues translated from the *por* and *vor* genes matched virtually every residue of the amino termini of the subunits determined by amino acid sequencing (Fig. 1), indicating that the subunits were correctly identified. Although amino-terminal sequence information was not available for the δ subunit of *P. furiosus* VOR, it was identified by the high similarity of the translated sequence to the N termini of other δ subunits (Fig. 1). The absence of an ATG codon indicates that the gene for the VOR δ subunit is translated from a GTG start codon (Fig. 1 and 5). Since the holoenzymes of both POR and VOR contain the γ subunit in equimolar amounts, three separate transcription units (of *porG*, *porDAB*, and *vorDAB*) are assumed to be responsible for the production of these two enzymes. This is supported by archaeal consensus transcriptional start and termination signal sequences in each case (Fig. 5) (13, 29, 39). The overall G+C content of the sequenced region was 42.8%; the G+C content of the *por*, *vor*, and *porG* genes was 43.8%.

FIG. 1. Multiple alignment of N-terminal amino acid sequences of 2-ketoacid ORs of hyperthermophiles, *H. halobium*, and *H. pylori*. The amino acid sequences are boxed according to their phylogenetic relationship. Conserved positions are shown in boldface. A comparison with the sequences as translated from the gene sequence is also included (denoted s). Arrows show residues from which oligonucleotides were derived for PCR amplification (plus or minus strand). Superscripts: a, the sequence published previously for the γ subunit of *T. maritima* POR (7, 31) is identical to the *P. furiosus* POR α subunit; b, position 211 of the large subunit of *H. halobium* POR, as shown in Fig. 3 and 4 (38); c, two mismatches occurred between the sequence as determined from the protein (italics and large dots) and the sequence translated from the gene; d, the sequences of *P. furiosus* POR and VOR γ subunits are identical (see Fig. 2); e, the newly determined N-terminal amino acid sequence for the γ subunit of *T. maritima* POR; f, position 1 of the large subunit of *H. halobium* POR (38). *Pf*, *P. furiosus*; *Tm*, *T. maritima*; *Tl*, *T. litoralis*; *Af*, *A. fulgidus*; *Hp*, *H. pylori*; *Hh*, *H. halobium*.

The regions flanking the POR and VOR genes (Fig. 2) were also sequenced. There was no indication of adjacent genes encoding IOR or KGOR. A three-reading-frame operon (termed *aca* for acetoacetyl-CoA synthase) and an incomplete one (termed *frx* for F_{420}-reducing hydrogenase) were identified upstream of *porG* (all on the complementary strand). The *frx* operon contained one gene (*frxA*) showing significant similarity to genes for proteins of unknown function associated with the F_{420}-reducing hydrogenase of methanogens (3, 14) and other hydrogenase-processing proteins (*hyaA* and *hoxM* [reviewed in reference 12]). The three-gene *aca* operon encoded proteins showing significant similarity to acyl carrier protein synthetases (*acaA*; e.g., accession number A42431) and eukaryotic sterol carrier proteins (*acaA* and *acaC*; e.g., accession number S34744 [36]). The significance of these similarities is unknown, but these putative gene products appear to be unrelated to the functions of POR and VOR.

T. maritima por. In contrast to *P. furiosus*, Southern hybridization with a probe for *T. maritima* POR (pTm-3) yielded only a single band in each lane of *T. maritima* genomic digests. A 4,055-bp *Pst*I-*Hin*dIII fragment was identified and cloned into pUC19 (pHP-511) and pBluescript (pKSHP). This coded for the δ, α, and β subunits and for the C-terminal part of γ subunit. An overlapping 3,418-bp *Bam*HI fragment was subsequently cloned into pBluescript II KS^+ to obtain the rest of the operon (pKB-112; Fig. 2). The inserts of both plasmids were completely sequenced (5,728 bp). The two fragments contained the entire *por* operon, which encodes the four POR subunits (*porG*, *porD*, *porA*, and *porB*; Fig. 2, 3, and 4). The amino-terminal sequences were virtually identical to those determined by amino acid sequencing of the separated subunits (including the newly determined sequence of the γ subunit), showing that the correct genes had been identified. Two mismatches occurred in the N terminus of the β subunit, one residue being added and in exchange two others being omitted (Fig. 1). No other reading frame with similarity to any of the

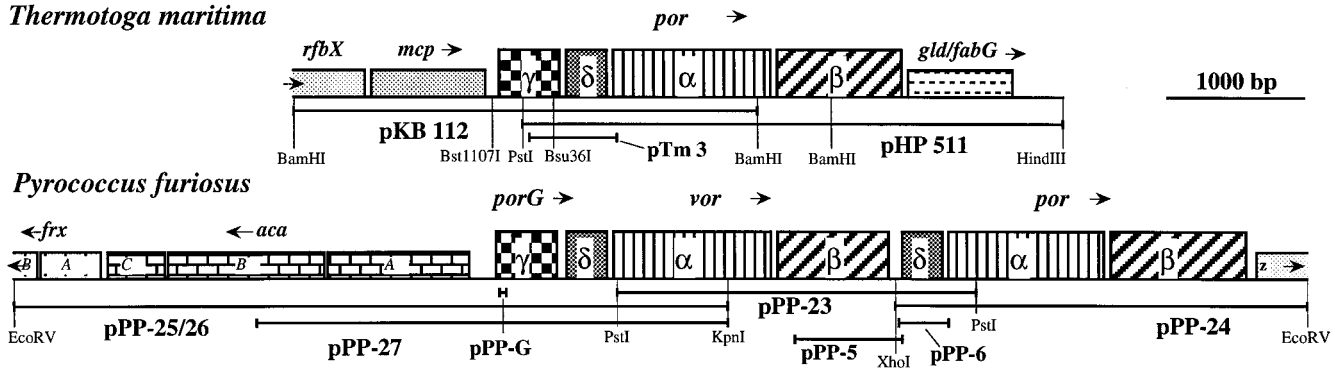

FIG. 2. Graphic representation of *P. furiosus* and *T. maritima* genomic fragments. The subunit organization of POR and VOR operons is indicated in tall boxes, and other genes and reading frames are shown in small boxes. The fragments pTM 3, pPP-5, pPP-6, and pPP-G were PCR amplified from oligonucleotides derived from the N-terminal amino acid sequences (Fig. 1) as described in Materials and Methods and were used for the identification and cloning of the genomic fragments. The gene designations are as follows: *rfbX*, open reading frame homologous to the CDP-abequose synthase gene; *mcp*, methyl-accepting chemotaxis protein gene; *gld*/*fabG*, glucose dehydrogenase/oxoacyl carrier protein reductase gene; *frxA*, gene for a protein homologous to *Methanobacterium thermoautotrophicum frhD* and *Methanococcus vannielii frcD* and *frxD* hydrogenase subunits; *frxB*, gene for an unknown putative transmembrane protein in the same operon; *acaA*, gene for a protein homologous to acyl carrier protein synthase (*fabH*); *acaB*, gene for a protein homologous to sterol carrier proteins and acetoacetyl-CoA synthases (*aca*); *acaC*, gene for a protein homologous to the C-terminal part of eucaryotic sterol carrier proteins; z, gene for an unknown protein.

subunits of the hyperthermophilic ORs was found upstream and downstream of *por*. The overall G+C content of the sequenced region was 48.8%; the G+C content of the *por* operon was 49.4%.

In addition to the *por* operon in *T. maritima*, three other genes were identified and sequenced, as shown in Fig. 2. Upstream were two genes that encoded proteins homologous to bacterial CDP-abequoses (*rbfJ*; accession number M29713) and methyl-accepting chemotaxis proteins (*mcp*; reviewed in reference 43), while immediately downstream was a gene (*gld*/*fab*) that encoded a protein with significant similarity to the superfamily of short-chain alcohol dehydrogenases, which also includes glucose dehydrogenases and oxoacyl carrier protein reductases (27). The *T. maritima gld*/*fab* gene is the first example of a hyperthermophilic member of this superfamily, although the nature of the oxidoreductase-type enzyme it encodes remains to be determined. For the present, we conclude that the genes surrounding the *T. maritima por* operon are unrelated to the function of POR.

Molecular properties of *P. furiosus* POR and VOR and *T. maritima* POR. The calculated molecular weights of the α, β, and δ subunits were, respectively, 44,186, 36,261, and 12,012 for *P. furiosus* POR and 43,960, 34,766, and 11,851 for *P. furiosus* VOR, and that of the common γ subunit was 20,033. The values for the α through δ subunits of *T. maritima* POR were 44,319, 36,385, 21,298, and 11,257, respectively. All of these values agree within 10% of the values obtained by sodium dodecyl sulfate (SDS) gel electrophoresis (7, 17), with the exception of the γ subunit of *P. furiosus* POR (24,000 from SDS gels). The calculated amino acid compositions of the three enzymes were likewise in good agreement with the composition based on chemical amino acid analysis. The one exception was the cysteine content of *P. furiosus* POR, which was underestimated by chemical analysis (8 versus 15 residues per αβγδ tetramer from the gene sequences [7]). *T. maritima* POR contained 13 cysteine residues per αβγδ tetramer (the analytical value was 15 [7]), while *P. furiosus* VOR contains 14 cysteine residues per αβγδ tetramer (this had not been determined chemically). Cysteine contents have important consequences for the predicted reaction mechanism, since a striking feature common to the sequences of all three ORs is the presence of two ferredoxin-type FeS cluster motifs in the small δ subunit (CXXCXXCXXXCP; PROSITE). In addition, four conserved cysteine residues were present in each of the β subunits, and these cysteines are assumed to coordinate a third FeS cluster in each enzyme. This subunit also contained a conserved TPP-binding domain (16, 30, 34). Thus, in the following calculations, it is assumed that each of the αβγδ tetramers contains three [4Fe-4S] clusters.

Sequence comparisons of *P. furiosus por* and *vor*, *T. maritima por*, and PORs from mesophiles. The sequences of the three ORs from the hyperthermophiles were remarkably similar (Table 1; Fig. 3, 4, and 6). Excluding the shared γ subunit, *P. furiosus* POR and VOR had 53% identical residues in the α, β, and δ subunits (60% identity at the nucleotide level). The identity scores were virtually the same for the three subunits (range: 52 to 54%); however, there were stretches of striking dissimilarity in several places. For example, the first 40 amino acids of the δ subunits were not homologous, while the remainder was almost identical. There were also two short stretches unique to the *P. furiosus* POR β subunit, one consisting of 7 amino acid residues and the second consisting of 12 (Fig. 4). On the other hand, the 60-amino-acid TPP-binding domains in the β subunits were virtually identical (54 identical residues out of 60; Fig. 4). The unexpected linkage of *P. furiosus* POR and VOR (and, judged from the N-terminal amino acid sequences, of *T. litoralis* POR and VOR; Fig. 1) can be explained by a partial operon duplication involving the δ, α, and β subunits ultimately leading to the creation of separate promoter structures for the shared γ subunit, for the *vor* operon, and for the *por* operon. Two partial gene fragments from *P. furiosus* had been previously entered in the databases. One encoded amino acid residues 59 to 150 of *P. furiosus porA* (bp 7163 to 7438, entry R7T7 in the DBEST library [39a]), and the reported sequence was identical to the one determined here. For the second partial sequence (193 bp; accession number T12789 [39a]), the first 160 bp is identical to the anticoding strand of *porA* (amino acid residues 193 to 240; bp 7565 to 7725; the last 33 bp is a vector sequence), but there are four mismatches and one reading frame error (additional C, position 148) in the reported sequence.

Both POR and VOR were equally similar to *T. maritima* POR, with 45% identity (for all four subunits; Table 1) and no preference for a particular subunit. On the nucleotide level, *P.*

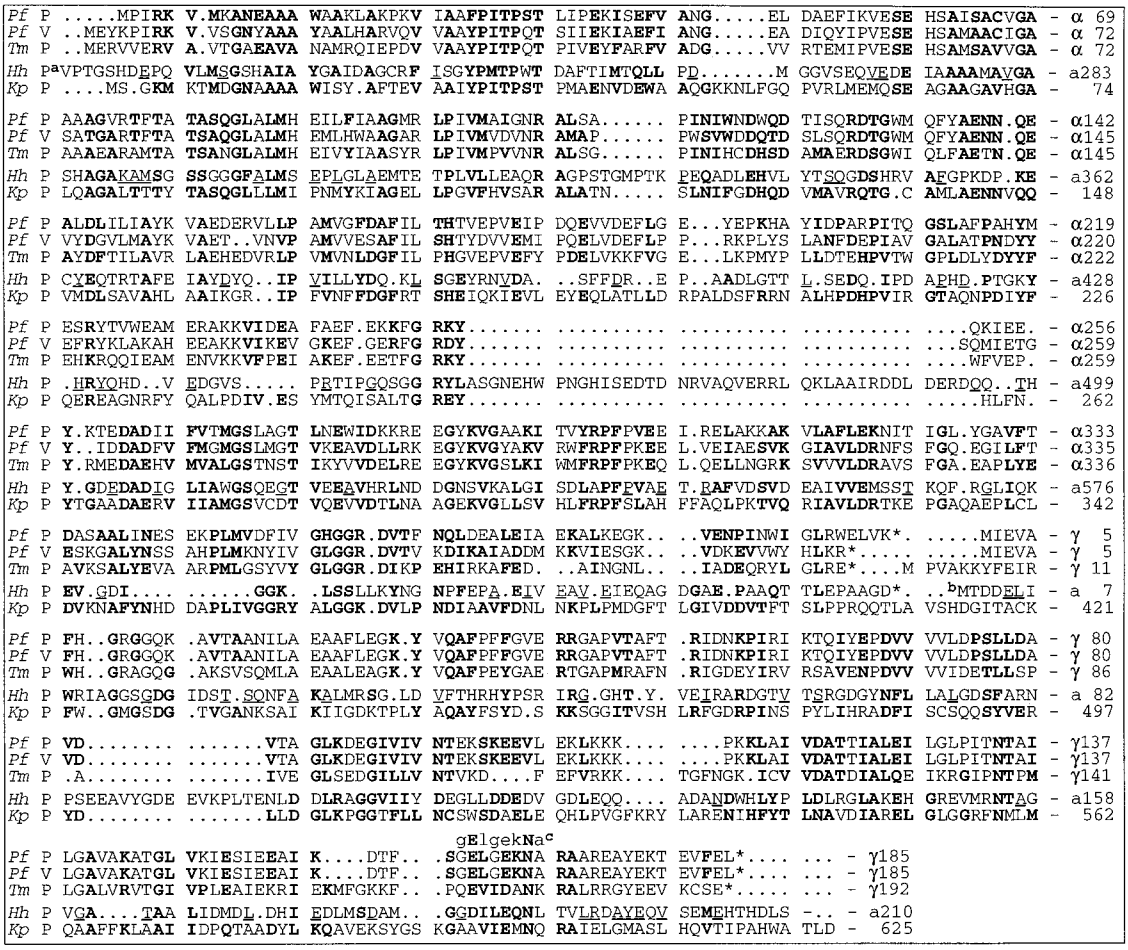

FIG. 3. Multiple alignment of the POR and VOR amino acid sequences: α and γ subunits. *P. furiosus* POR (*Pf* P) and VOR (*Pf* V) and *T. maritima* POR α subunit (*Tm* P) are aligned with *H. halobium* POR (*Hh* P) (superscript a, alignment starts at position 211 of the large subunit; superscript b, alignment starts at position 1 of the large subunit), and *K. pneumoniae* POR (*Kp* P). The amino acid sequences of the PORs from *E. agglomerans*, *R. rubrum*, and an *Anabaena* sp. and of *T. vaginalis* POR A and POR B were not included because of the high degree of similarity to the ones shown (Table 1 and Fig. 6). The complete alignment of the six sequences of the single-subunit PORs is published in reference 18. The alignment is continued in Fig. 4 (δ and β subunits) with the sequences of the single-subunit ORs extending throughout without any gaps. Positions conserved between any of the *H. halobium*, *P. furiosus*, and *T. maritima* ORs and the bacterial, single-subunit POR are shown in boldface. Positions that are conserved in *H. halobium* POR and any of the three ORs of the hyperthermophiles are underlined. Gaps are indicated by dots. For references and accession numbers, see Materials and Methods. Superscript c, aldehyde dehydrogenase active-site motif as found in a search in the PROSITE database (the glutamate is an active site residue in these enzymes); *, stop codon.

furiosus por and *vor* operons were 53 and 54% identical to *T. maritima por*, respectively. The high similarity among both POR and VOR from *P. furiosus* and POR from *T. maritima* was unexpected (Table 1 and Fig. 3, 4, and 6), given the phylogenetic distance between these organisms (49). However, the presence of a similar, four-subunit POR in the mesophilic bacterium *H. pylori* points to more general distribution of this type of 2-ketoacid OR in bacteria (20).

Database sequences of the PORs from mesophilic bacteria (often termed *nifJ* genes) and from the amitochondriate protist *T. vaginalis* were very similar to the *P. furiosus* and *T. maritima* ORs, as suggested previously (18, 28). In fact, the different subunits of the hyperthermophilic ORs were homologous to discrete domains in the single large subunit (A) of the mesophilic PORs (Fig. 7). Note that the latter have a molecular weight of about 130,000, which is slightly larger than the sum of the four subunits (α, β, γ, and δ) of the *T. maritima* and *P. furiosus* enzymes. Hence, the α subunit of the hyperthermophilic ORs aligned to the N-terminal (or α) domain of the A subunit. This was followed by the γ domain, the δ domain (containing the two ferredoxin-type FeS cluster motifs), and finally, with one additional 60-amino-acid insertion not present in the hyperthermophilic ORs, the β domain (containing the third FeS cluster and the TPP-binding site; Fig. 4). In all cases examined, these domains were identified by computer-aided multiple alignments (PILEUP) without applying any bias. The pairwise identity scores were between 25 and 28% when the four subunits of the *P. furiosus* and *T. maritima* enzymes were aligned in a single sequence (αγδβ) and compared with the single subunit of the mesophilic PORs (Table 1 and Fig. 7). An alignment of the amino acid sequences of *P. furiosus* VOR and the PORs from *T. maritima*, *H. halobium*, and *K. pneumoniae* is given in Fig. 3 and 4. The sequences are arranged in the domain order (α-γ-δ-β) found in the large, single-subunit (A) PORs.

The scenario of recombination events proposed for the single-subunit ORs and also for the two-subunit IORs of *P. furiosus* and *T. litoralis* is more complicated. For the single-subunit enzymes, at least two separate events have to be assumed. First, a γ-δ fusion must have occurred in the original,

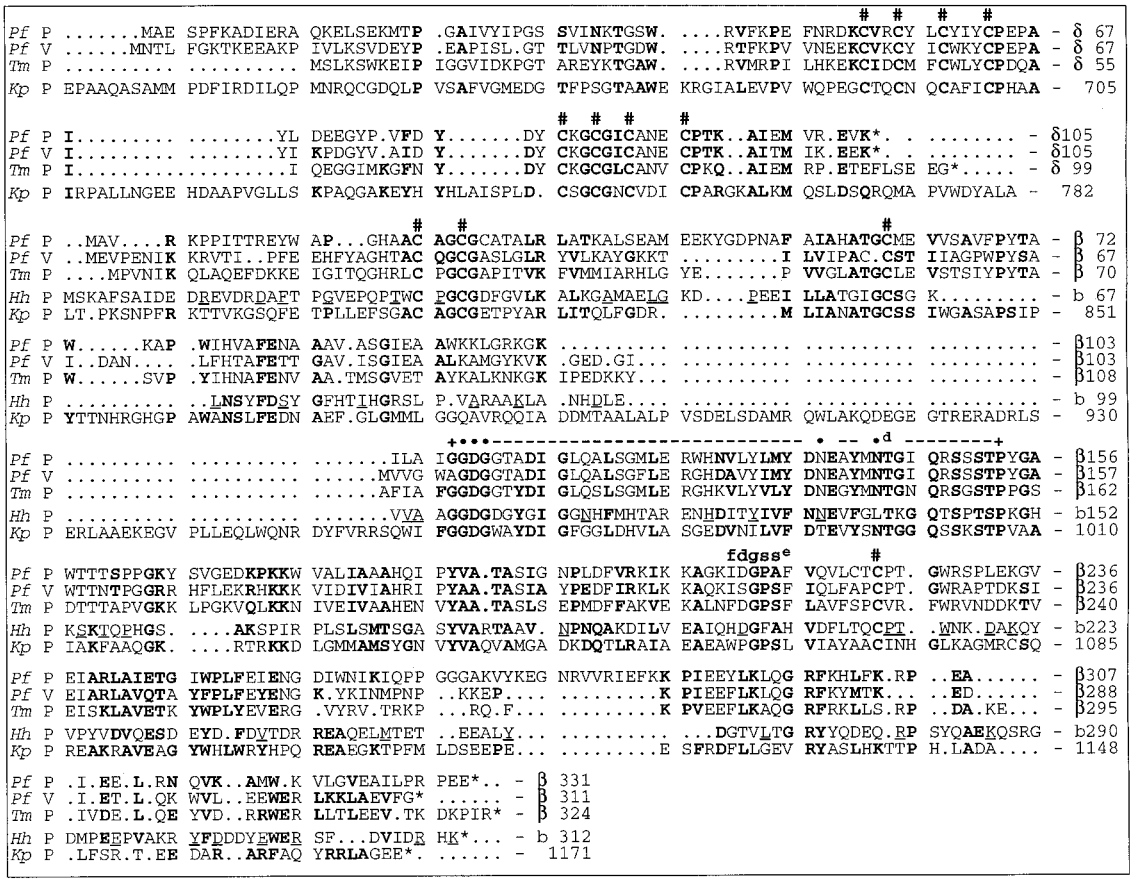

FIG. 4. Multiple alignment of the POR and VOR amino acid sequences. Continuation of the alignment from Fig. 3, including the δ and β subunits of *P. furiosus* POR and VOR and *T. maritima* POR. #, conserved cysteine residues forming two ferredoxin-type FeS-cluster motifs of the δ subunit (CXXCXXCXXXCP) and the conserved cysteines of the β subunit; superscript d, the TPP-binding domain (+---+) conserved in all TPP-containing enzymes (16, 30, 34), including a GDG motif (●), a conserved Asn-Thr (a possible replacement for the missing Asn residue in *H. halobium* POR is also indicated); superscript e, glutamine synthase active-site motif as found in a search with *T. maritima* POR β subunit in the PROSITE database. For other abbreviations and symbols, see the legend to Fig. 3.

four-subunit γδαβ operon. Second, there must have occurred a recombination event that resulted in the insertion of the combined γ-δ-subunit gene between the genes for the α and β subunits (Fig. 7). Although the primary structure of IOR is not available, we postulate that its large subunit arose by a recombination event similar to that of the single-subunit ORs but that only the δ subunit was integrated between the α and β subunits. The γ subunit remained as a second, smaller IOR subunit (Fig. 1 and 7). The presence of more than four FeS clusters per IOR holoenzyme (or two per A-B dimer [31, 32]) shows that it does not lack the δ domain, as is the case with *H. halobium* POR (see below). However, on the basis of the molecular weight estimated by SDS gel analysis, the large subunit of IOR is about 200 residues smaller than would be expected from a direct α-δ-β fusion, suggesting a partial deletion in the course of the recombination event (Fig. 7).

It had been previously shown that the two-subunit (a-b) POR of the aerobic mesophilic archaeon *H. halobium* con-

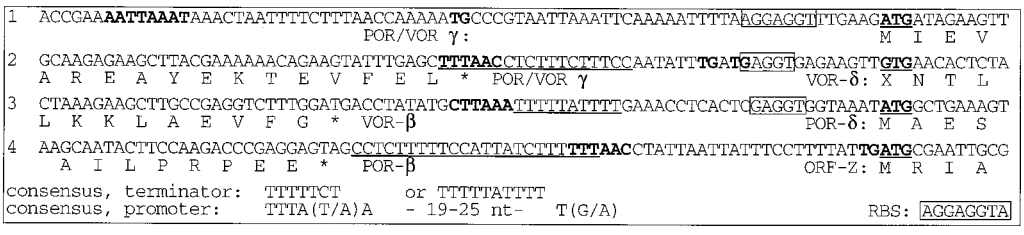

FIG. 5. Nucleotide sequences between *P. furiosus* POR and VOR genes and putative signal sequences. The sequences are aligned at the start codon of the downstream gene (boldfaced and underlined; *P. furiosus* VOR is translated from a GTG). Putative box A and box B sites are shown in boldface. Transcription usually starts on the G or A site of box B (13). Pyrimidine-rich consensus transcriptional termination signal sequences (29, 39) are underlined, and ribosomal binding sites derived from the 3′ end of the *P. furiosus* 16S rRNA (RBS) (accession number U20163) (1) are boxed. Sequences: 1, promoter region of *porG* (upstream is an AT-rich noncoding region [bp 3325 to 3562; Fig. 2]); 2, promoter region of *P. furiosus vor*; 3, promoter region of *P. furiosus por* (no meaningful box B motif was identified); and 4, terminator region of *P. furiosus por* and promoter of open reading frame Z (ORF-Z) (no RBS identified; Fig. 2). nt, nucleotides.

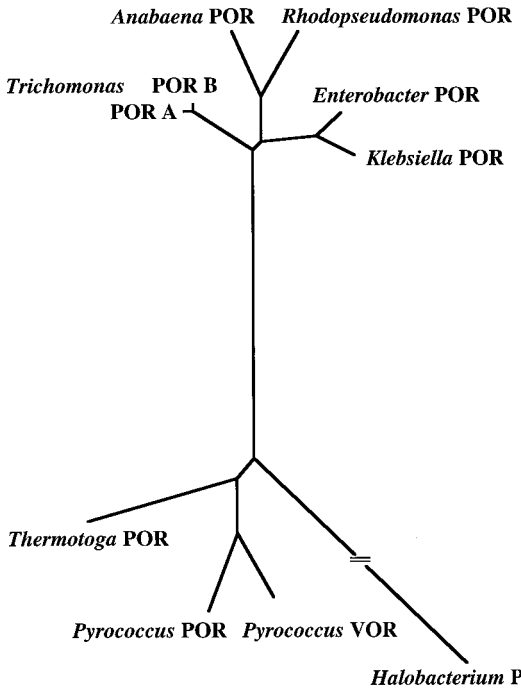

FIG. 6. Phylogenetic dendrogram of PORs and VOR, calculated from the multiple alignment as shown in Fig. 3 and 4 with the other POR sequences included. For the calculation only 742 positions without gaps out of a total of 1,385 residues were used. The branch lengths denote relative distances, and the *H. halobium* POR branch length is approximately double what is shown. Note that the dendrogram reflects distances between individual molecules evolved separately after gene recombination events (Fig. 7) and not the organisms themselves.

tained a conserved TPP-binding site in its smaller (b) subunit in a part of the subunit that was similar to the C-terminal part of the large single A subunit of the bacterial PORs (Fig. 4 and 7) (16, 18, 38). Also, conserved cysteine residues were found near the N terminus of the subunit (20, 28, 38). However, the large subunit (a) of *H. halobium* POR could not be aligned with the bacterial PORs in a meaningful way in these studies. A detailed analysis of the alignments among the four subunits of the ORs from *P. furiosus* and *T. maritima* with the *H. halobium* enzyme clearly showed that the first third of the large subunit (a) of *H. halobium* POR corresponds to the γ subunits from the hyperthermophilic enzymes, while the remaining two-thirds is homologous to the α subunits (Fig. 3, 4, and 7). Thus, the domain order observed in the single large subunit (A) of the bacterial PORs (α to γ) is reversed in the *H. halobium* POR a subunit (γ to α). Similar alignment analyses showed, as anticipated, that the *H. halobium* POR b subunit is homologous to the *P. furiosus* and *T. maritima* β subunits. We were unable to find in *H. halobium* POR any sequence that resembled the δ subunits of the hyperthermophilic enzymes. By analogy to the operon duplication in *P. furiosus*, it is proposed that the large subunit (a) of *H. halobium* POR arose by the deletion of the δ subunit from a γ-δ-α precursor, leading to the formation of a subunit composed of the γ and α domains, while the β-subunit directly gave rise to the smaller b subunit of *H. halobium* POR (Fig. 7). Since this contains four conserved cysteine residues to coordinate just one FeS cluster, it readily explains why the *H. halobium* enzyme contains only two FeS clusters per holoenzyme ($\alpha_2\beta_2$). The overall similarity of *H. halobium* POR to both the mesophilic single-subunit (A) enzymes and the four hyperthermophilic subunits was only about 21%. For example, there are 40 amino acids in the α domain of the large a subunit of *H. halobium* POR that have no equivalent (Fig. 3).

A significance evaluation of the unbiased pairwise alignments with *H. halobium* POR did not yield scores much different from random scores, in contrast to the comparisons among all other ORs. However, this was not the case when the evaluation was performed with the *H. halobium* POR sequence aligned as described above (Table 1). Many conserved signatures were identified throughout all of the OR sequences, and those shared by the *H. halobium* POR sequence and the subunits of the hyperthermophilic ORs served to confirm the domain assignment in the former enzyme (Fig. 3 and 4). The inclusion of the *H. halobium* sequence into the multiple alignment requires that the large a subunit of *H. halobium* POR be split at position 210 to accommodate the homologous domains.

The multiple alignment presented in Fig. 3 and 4 was obtained by including each of the six known single-subunit POR sequences (for a multiple alignment of those, see reference 18), but for reasons of simplicity, only one is shown. However, these PORs were included in pairwise comparisons (Table 1) and in the construction of the phylogenetic dendrogram which

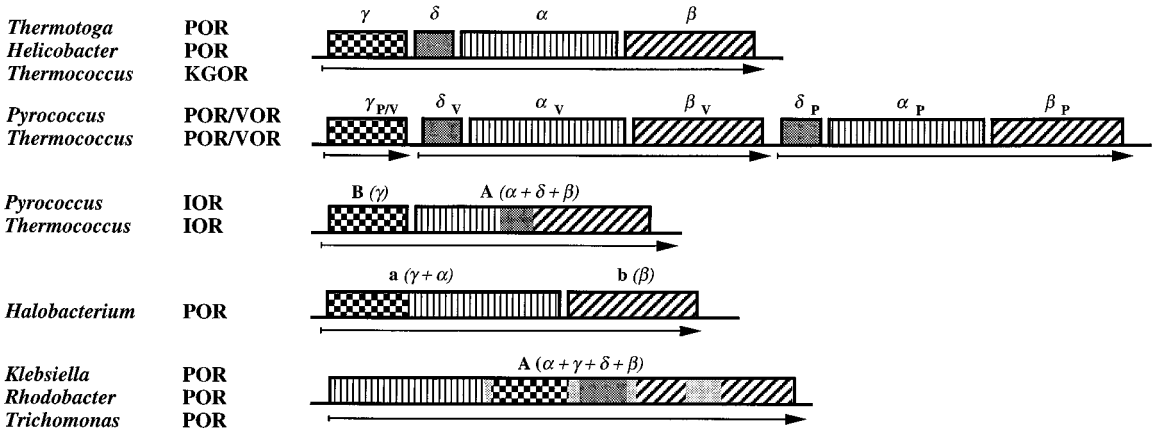

FIG. 7. Comparison of the subunit and domain structures of the 2-ketoacid ORs. The structures of *P. furiosus* and *T. litoralis* IORs are predicted. Homologous domains are shown in the same shading. It is assumed that *P. furiosus* and *T. litoralis* IORs have lost a part of the α domain in the recombination event (see text). The arrows indicate predicted transcriptional units.

used 742 positions without gaps (Fig. 6). The multiple alignment showed a considerable number of conserved residues. These encompass 14 different amino acids, and besides 12 cysteines, the most abundant are glycine ($n = 12$) and proline ($n = 7$) (data not shown). Although most of them cannot be assigned a function in the absence of crystallographic data, it seems reasonable to conclude that the eight cysteine residues in the δ domain and the four cysteine residues in the β domain coordinate a total of three FeS clusters in all of the enzymes, except for *H. halobium* POR, which lacks the δ domain. Similarly, the TPP-binding site in the β domain is highly conserved in all ORs.

Thus, the evolution of all of the various 2-ketoacid oxidoreductases, whether they comprise one, two, or four different subunits, can be explained by the rearrangement of four ancestral genes of the type now present in *T. maritima* POR, *P. furiosus* VOR, and *P. furiosus* POR. The two-subunit archaeal enzymes (*P. furiosus* IOR and *H. halobium* POR) and the single-subunit mesophilic enzymes may have originated in one or more of the gene duplication and recombination events described above and subsequently evolved as a separate phylogenetic unit.

ACKNOWLEDGMENTS

This research was supported by grants from the Department of Energy (FG09-88ER13901) and the Office of Naval Research (N00014-90-J-1894).

We are grateful to Ivan Hrdy and Miklós Müller for providing unpublished sequence data, and we thank them and Johannes Heider, Xuhong Mai, Marc F. J. M. Verhagen, Ulrike Harms, and Andrea Hutchins for many helpful discussions.

REFERENCES

1. **Achenbach, L. A.** Unpublished data.
1a. **Adams, M. W. W.** 1993. Enzymes and proteins from organisms that grow near and above 100°C. Annu. Rev. Microbiol. **47:**627–658.
2. **Adams, M. W. W.** 1994. Biochemical diversity among sulfur-dependent, hyperthermophilic microorganisms. FEMS Microbiol. Rev. **15:**261–277.
3. **Alex, L. A., J. N. Reeve, W. H. Orme-Johnson, and C. T. Walsh.** 1990. Cloning, sequencing, and expression of the genes encoding the subunits of the nickel-containing 8-hydroxy-5-deazaflavin reducing hydrogenase from *Methanobacterium thermoautotrophicum* ΔH. Biochemistry **29:**7237–7244.
4. **Arnold, W., A. Rump, W. Klipp, U. Priefer, and A. Pühler.** 1988. Nucleotide sequence of a 24,206-base-pair DNA fragment carrying the entire nitrogen fixation gene cluster of *Klebsiella pneumoniae*. J. Mol. Biol. **203:**715–738.
5. **Bauer, C. C., L. Scappino, and R. Haselkorn.** 1993. Growth of the cyanobacterium *Anabaena* on molecular nitrogen: *NifJ* is required when iron is limited. Proc. Natl. Acad. Sci. USA **90:**8812–8816.
6. **Blamey, J. M., and M. W. W. Adams.** 1993. Purification and characterization of pyruvate ferredoxin oxidoreductase from the hyperthermophilic archaeon *Pyrococcus furiosus*. Biochim. Biophys. Acta **1161:**19–27.
7. **Blamey, J. M., and M. W. W. Adams.** 1994. Characterization of an ancestral type of pyruvate ferredoxin oxidoreductase from the hyperthermopilic bacterium, *Thermotoga maritima*. Biochemistry **33:**1000–1007.
8. **Brostedt, E., and S. Nordlund.** 1991. Purification and partial characterization of a pyruvate oxidoreductase from the photosynthetic bacterium *Rhodospirillum rubrum* grown under nitrogen-fixing conditions. Biochem. J. **279:**155–158.
9. **Cannon, M., F. Cannon, V. Buchanan-Wollaston, D. Alley, A. Alley, and J. Beyon.** 1988. The nucleotide sequence of the *nifJ* gene of *Klebsiella pneumoniae*. Nucleic Acids Res. **16:**11379.
10. **Docampo, R., S. N. J. Moreno, and R. P. Mason.** 1987. Free radical intermediates in the reaction of pyruvate:ferredoxin oxidoreductase in *Trichomonas foetidus* hydrogenosomes. J. Biol. Chem. **262:**12417–12420.
11. **Fiala, G., and K. O. Stetter.** 1986. *Pyrococcus furiosus* sp. nov. represents a novel genus of marine heterotrophic archaebacteria growing optimally at 100°C. Arch. Microbiol. **145:**56–61.
12. **Friedrich, B., and E. Schwartz.** 1993. Molecular biology of hydrogen utilization in aerobic chemolithotrophs. Annu. Rev. Microbiol. **47:**351–385.
13. **Hain, J., U. Hüdepohl, and W. Zillig.** 1992. Elements of an archaeal promoter defined by mutational analysis. Nucleic Acids Res. **20:**5423–5428.
14. **Halboth, S., and A. Klein.** 1992. *Methanococcus voltae* harbors four gene clusters potentially encoding two [NiFe] and two [NiFeSe] hydrogenases, each of the cofactor F_{420}-reducing or F_{420}-non-reducing types. Mol. Gen. Genet. **233:**217–224.
15. **Harms, U., and M. W. W. Adams.** Unpublished data.
16. **Hawkins, C. F., A. Borges, and R. N. Perham.** 1989. A common structural motif in thiamine pyrophosphate-binding enzymes. FEBS Lett. **255:**77–82.
17. **Heider, J., X. Mai, and M. W. W. Adams.** Characterization of 2-ketoisovalerate ferredoxin oxidoreductase, a new and reversible coenzyme A-dependent enzyme involved in peptide fermentation by hyperthermophilic archaea. J. Bacteriol., in press.
18. **Hrdy, I., and M. Müller.** 1995. Primary structure and eubacterial relationships of the pyruvate:ferredoxin oxidoreductase of the amitochondriate eukaryote, *Trichomonas vaginalis*. J. Mol. Evol. **41:**388–396.
19. **Huber, R., T. A. Langworthy, H. König, M. Thomm, C. R. Woese, U. B. Sleytr, and K. O. Stetter.** 1986. *Thermotoga maritima* sp. nov. represents a new genus of unique extremely thermophilic eubacteria growing up to 90°C. Arch. Microbiol. **144:**324–333.
20. **Hughes, N. I., P. A. Chalk, C. L. Clayton, and D. J. Kelly.** 1995. Identification of carboxylation enzymes and characterization of a novel four-subunit pyruvate:flavodoxin oxidoreductase from *Helicobacter pylori*. J. Bacteriol. **177:**3953–3959.
21. **Juszczak, A., S. Aono, and M. W. W. Adams.** 1991. The extremely thermophilic eubacterium, *Thermotoga maritima*, contains a novel iron-hydrogenase whose cellular-activity is dependent upon tungsten. J. Biol. Chem. **266:**13834–13841.
22. **Kelly, R. M., and M. W. W. Adams.** 1994. Metabolism in hyperthermophilic microorganisms. Antonie van Leeuwenhoek J. Microbiol. **66:**247–270.
23. **Kerscher, L., and D. Oesterhelt.** 1981. Purification and properties of 2-oxoacid:ferredoxin oxidoreductases from *Halobacterium halobium*. Eur. J. Biochem. **116:**587–594.
24. **Kerscher, L., and D. Oesterhelt.** 1981. The catalytic mechanism of 2-oxoacid: ferredoxin oxidoreductases from *Halobacterium halobium*. One-electron transfer at two distinct steps of the catalytic cycle. Eur. J. Biochem. **116:**595–600.
25. **Kletzin, A.** 1992. Molecular characterisation of a DNA ligase gene of the extremely thermophilic archaeon *Desulfurolobus ambivalens* shows close phylogenetic relationship to eukaryotic ligases. Nucleic Acids Res. **20:**5389–5396.
26. **Kreutzer, R., S. Dayananda, and W. Klingmüller.** 1991. Cotranscription of the electron transport protein genes *nifJ* and *nifF* in *Enterobacter agglomerans* 333. J. Bacteriol. **174:**6822–6830.
27. **Krozowski, Z.** 1994. The short-chain alcohol dehydrogenase superfamily: variations on a common theme. J. Steroid Biochem. Mol. Biol. **51:**125–130.
28. **Kunow, J., D. Linder, and R. K. Thauer.** 1995. Pyruvate:ferredoxin oxidoreductase from the sulfate-reducing *Archaeoglobus fulgidus*: molecular composition, catalytic properties, and sequence alignments. Arch. Microbiol. **163:**21–28.
29. **Lechner, K., G. Heller, and A. Böck.** 1989. Organisation and nucleotide sequence of a transcriptional unit of *Methanococcus vannielii* comprising genes for protein synthesis elongation factors and ribosomal proteins. J. Mol. Evol. **29:**20–27.
30. **Lindqvist, Y., and G. Schneider.** 1993. Thiamine pyrophosphate-dependent enzymes: transketolase, pyruvate oxidase and pyruvate decarboxylase. Curr. Opin. Struct. Biol. **3:**896–901.
31. **Mai, X., and M. W. W. Adams.** 1994. Indolepyruvate ferredoxin oxidoreductase from the hyperthermophilic archaeon *Pyrococcus furiosus*. J. Biol. Chem. **269:**16726–16732.
32. **Mai, X., and M. W. W. Adams.** Unpublished data.
33. **Meinicke, B., J. Bertram, and G. Gottschalk.** 1987. Purification of the pyruvate-ferredoxin oxidoreductase from *Clostridium acetobutylicum*. Arch. Microbiol. **152:**244–250.
34. **Muller, Y. A., Y. Lindqvist, W. Furey, G. E. Schulz, F. Jordan, and G. Schneider.** 1993. A thiamine diphosphate binding fold revealed by comparison of the crystal structures of transketolase, pyruvate oxidase and pyruvate decarboxylase. Structure **1:**95–103.
35. **Neuner, A., H. W. Jannasch, S. Belkin, and K. O. Stetter.** 1990. *Thermococcus litoralis* sp. nov.: a new species of extremely thermophilic, marine archaebacterium. Arch. Microbiol. **153:**205–207.
36. **Pfeifer, S. M., N. Sakuragi, A. Ryan, A. L. Johnson, R. G. Deeley, J. T. Billheimer, M. E. Baker, and J. F. Strauss III.** 1993. Chicken sterol carrier protein 2/sterol carrier protein x: cDNA cloning reveals evolutionary conservation of structure and regulated expression. Arch. Biochem. Biophys. **304:**287–293.
37. **Pieulle, L., B. Guigliarelli, M. Asso, F. Dole, A. Bernadac, and E. C. Hatchikian.** 1995. Isolation and characterization of the pyruvate-ferredoxin oxidoreductase from the sulfate-reducing bacterium *Desulfovibrio africanus*. Biochim. Biophys. Acta **1250:**49–59.
38. **Plaga, W., F. Lottspeich, and D. Oesterhelt.** 1992. Improved purification crystallization and primary structure of pyruvate:ferredoxin oxidoreductase from *Halobacterium halobium*. Eur. J. Biochem. **205:**391–397.
39. **Reiter, W.-D., P. Palm, and W. Zillig.** 1988. Transcription termination in the archaebacterium Sulfolobus: signal structures and linkage to transcription initiation. Nucleic Acids Res. **16:**2445–2459.
39a. **Robb, F. T.** 1993. Unpublished data.

40. **Sambrook, J., E. F. Fritsch, and T. Maniatis.** 1989. Molecular cloning: a laboratory manual, 2nd ed. Cold Spring Harbor Laboratory Press, Cold Spring Harbor, N.Y.
41. **Smith, E. T., J. M. Blamey, and M. W. W. Adams.** 1994. Pyruvate ferredoxin oxidoreductases of the hyperthermopilic archaeon, *Pyrococcus furiosus*, and the hyperthermophilic bacterium, *Thermotoga maritima*, have different catalytic mechanisms. Biochemistry **33:**1008–1016.
42. **Stetter, K. O., G. Fiala, G. Huber, R. Huber, and G. Segerer.** 1990. Hyperthermophilic microorganisms. FEMS Microbiol. Rev. **75:**117–124.
43. **Stock, J. B., M. G. Surette, W. R. McCleary, and A. M. Stock.** 1992. Signal transduction in bacterial chemotaxis. J. Biol. Chem. **267:**19753–19756.
44. **Uyeda, K., and J. C. Rabinowitz.** 1971. Pyruvate-ferredoxin oxidoreductase. I. Purification and properties of the enzyme. J. Biol. Chem. **246:**3111–3119.
45. **Wahl, R. C., and W. H. Orme-Johnson.** 1987. Clostridial pyruvate oxidoreductase and the pyruvate-oxidizing enzyme specific for nitrogen fixation in *Klebsiella pneumoniae* are similar enzymes. J. Biol. Chem. **262:**10489–10496.
46. **Wieland, O. H.** 1983. The mammalian pyruvate dehydrogenase complex: structure and regulation. Rev. Biochem. Physiol. Pharmacol. **96:**123–170.
47. **Williams, K., P. N. Lowe, and P. F. Leadlay.** 1987. Purification and characterization of pyruvate:ferredoxin oxidoreductase from the anaerobic protozoon *Trichomonas vaginalis*. Biochem. J. **246:**529–536.
48. **Wilson, K.** 1990. Preparation of genomic DNA from bacteria, p. 2.4.1–2.4.5. *In* F. M. Ausubel, R. Brent, R. E. Kingston, et al. (ed.), Current protocols in molecular biology. John Wiley & Sons, Inc., New York.
49. **Woese, C. R., O. Kandler, and M. L. Wheelis.** 1990. Toward a natural system of organisms: proposal for the domains *Archaea*, *Bacteria*, and *Eukarya*. Proc. Natl. Acad. Sci. USA **87:**4576–4579.